Available online at www.sciencedirect.com
ScienceDirect
Journal of Membrane Science 296 (2007) 147–155
journal of MEMBRANE SCIENCE
www.elsevier.com/locate/memsci

Dextran fouling of polyethersulfone ultrafiltration membranes—Causes, extent and consequences

Heru Susanto [a,1], Steffen Franzka [b], Mathias Ulbricht [a,*]

[a] *Lehrstuhl für Technische Chemie II, Universität Duisburg-Essen, 45117 Essen, Germany*
[b] *Institut für Physikalische Chemie, Universität Duisburg-Essen, 45141 Essen, Germany*

Received 2 February 2007; received in revised form 8 March 2007; accepted 12 March 2007
Available online 19 March 2007

Abstract

In a recent paper [Susanto, Ulbricht, J. Membr. Sci. 266 (2005) 132], we showed that dextran does foul polyethersulfone (PES) ultrafiltration (UF) membranes by contact of the solution with the membrane surface without flux through the membrane. In this work, dextran fouling was visualized using atomic force microscopy (AFM) and quantified by ATR-IR spectroscopy and by the mass balance in simultaneous diffusion–adsorption measurements (SDAM). Good correlations have been found between the water flux reduction due to dextran adsorption and the quantitative data for bound dextran on the PES membranes. Further, a pronounced effect of dextran size on adsorptive membrane fouling was identified. Contact angle and zeta potential measurements with non-porous films, where solute entrapment in pores can be ruled out, gave additional clear evidence for dextran binding on the PES surface. Complementary data for adsorption and fouling of porous membranes and non-porous films by the protein myoglobin indicated that the larger fouling tendency for protein than for dextran is due to a higher surface coverage of PES by the adsorbed biomacromolecule layer. Data for batch UF confirm the conclusions from the static contact experiments because significant fouling is observed for PES membranes (more severe for myoglobin than for dextrans), while no fouling is seen for a cellulose-based UF membrane with the same nominal cut-off. Finally, two mechanisms for the attractive PES–dextran interaction – multiple hydrogen bonding involving the SO_2 groups of PES and "surface dehydration" of the relatively hydrophobic PES – are discussed.

Keywords: Ultrafiltration; Fouling; Polysaccharides; Dextran; Protein; Myoglobin; Adsorption

1. Introduction

Along with the increasing number and scale for applications of UF, studies of polysaccharide fouling of polymeric membranes have become an important issue. Such investigations were concerned with extracellular polysaccharides (EPS) [2,3], wine polysaccharides [4] or juice polysaccharides [5]. Recently, it was also found that there were significant interactions between UF membranes and fluorescent-labeled dextrans, with a reduced permeability and a changed retention of the membranes as consequences; but the causes were not identified [6]. In all the previously mentioned examples, it is probable that the interactions between the polysaccharide and the polymeric membrane were driven by "sticky" charged or hydrophobic groups conjugated with the carbohydrate. With unmodified and neutral dextran, which is commonly used for the characterization of UF membranes, there were considerable disagreements between different investigators on the question whether dextran fouls or does not foul UF membranes [7,8]. However, we have clearly shown that dextran – by contact of an aqueous solution with the membrane surface without any flux through the membrane – fouled commercial PES UF membranes (nominal cut-off 10 kg/mol) but did not foul commercial cellulose-based UF membranes with similar cut-off [1]. That result is supported by the recent study of Kweon and Lawler [9]. They reported that dextran fouls polysulfone UF membranes. However, the mechanism of the membrane–dextran interaction is still not clear. Furthermore, quantifications of the amounts of dextran attached to the membrane and of the factors affecting the fouling are also still missing.

In the present study, we focus on the visualization of dextran fouling by AFM and the quantification of dextran amounts

* Corresponding author. Tel.: +49 201 183 3151; fax. +49 201 183 3147.
E-mail address: mathias.ulbricht@uni-due.de (M. Ulbricht).
[1] Permanent address: Department of Chemical Engineering, Universitas Diponegoro, Indonesia.

0376-7388/$ – see front matter © 2007 Elsevier B.V. All rights reserved.
doi:10.1016/j.memsci.2007.03.027

attached on PES UF membranes by IR spectroscopy and the mass balance from SDAM. In addition to various dextrans with different average molar mass, a relatively small protein (myoglobin, with molar mass of 16.7 kg/mol) was also used (as "benchmark") in order to further estimate the extent and driving force for the adsorptive dextran fouling. Adsorption experiments with non-porous PES films were performed to clarify the mechanism of interaction. The results of this study demonstrate that adsorptive fouling of PES UF membranes by dextran is significant and, hence, they contribute to a better understanding of polysaccharide fouling and its consequences for ultrafiltration performance.

2. Materials and methods

2.1. Materials

Two commercial polyethersulfone (PES) membranes (GR81PP and SG146.39) donated by Alfa Laval, Denmark, and Sartorius, Germany, and one commercial cellulose-based membrane obtained from Sartorius (SC144.39 "Hydrosart"; as a reference) were used. Important characteristics for the original membranes are given in Table 1. All membranes have a nominal cut-off of 10 kg/mol. Fresh membranes were used in all experiments. To avoid the effect of membrane sample variability, the initial pure water flux (cf. Section 2.3) was used as a selection criterion, i.e. only membrane samples that had initial water permeability in the range ±10% relative to the average values were used for the experiments (cf. [1] for the selection procedure). Before use, the membranes were soaked overnight in water to remove impurities from the manufacturing process or additives used for stabilization. Dextran T-4, T-15, T-35, T-100 and T-200 (the numbers indicating molar mass in kg/mol) from Serva Feinbiochemica GmbH&Co., Heidelberg, Germany, and dextran T-10 and T-70 from Pharmacia Fine Chemicals, Uppsala, Sweden, were used as polysaccharides. Myoglobin from horse skeletal muscle (95–100% purity) was from Sigma–Aldrich Chemie GmbH, Steinheim, Germany. The myoglobin solutions (in phosphate buffer pH 7) were always freshly prepared and then pre-filtered through a 0.45 μm microfiltration membrane (Sartorius, Germany) to remove suspended material. Potassium dihydrogen phosphate (KH_2PO_4) and disodium hydrogen phosphate dihydrate ($Na_2HPO_4{\cdot}2H_2O$) were purchased from Fluka Chemie AG (Buchs, Germany). Nitrogen gas from Messer Griesheim GmbH, Krefeld, Germany, was of ultrahigh purity. Water purified with a Milli-Q system from Millipore was used for all experiments. Non-porous PES films were prepared by spin-coating (SCI-30 spin coater, LOT Oriel) of glass coverslips with solutions of PES (1%, w/w, in methylene chloride) at 523.6 rad/s (5000 rpm) for 1 min and subsequent drying overnight at ∼60 °C (cf. [10] for more details).

2.2. Dextran and protein analyses

The concentration of dextran as well as the molar mass distribution in solution was analyzed using gel permeation chromatography (GPC). A "Suprema" (PSS, Mainz, Germany) and a "Hema 40" (MZ Analytik, Mainz, Germany) column in series were used. Calibrations were performed using different dextran molar mass standards (PSS). The concentration of myoglobin was determined from its UV absorbance at 230 nm measured using the UV–vis spectrophotometer CARY-50 Probe (Varian, Germany).

2.3. Water flux measurement, adsorptive fouling and ultrafiltration procedures

The experimental set-up and procedures for analyzing membrane–solute interactions (adsorptive fouling) and membrane–solute–solute interactions (UF) have already been described in detail in the previous work [1]. Briefly, the experiments were carried out using a dead-end filtration system (Amicon cell models 8010 and 8050, for adsorptive fouling and UF experiments, respectively). Relative flux reduction (cf. Eq. (1)) was calculated by measuring the water flux at the same pressure (300 kPa for adsorptive fouling, either 20 or 40 kPa for UF) before and after fouling experiments. For static adsorption experiments, a solution of either dextran or myoglobin was added to the cell and the outer membrane surface was exposed for 3 h without any flux at a stirring rate of 31.416 rad/s (300 rpm). Afterwards, the solution was removed, and the membrane surface was rinsed two times by filling the cell with pure water (5 mL) and shaking it for 30 s. The UF of dextran (1 g/L) and protein (0.1 g/L, pH 7 in phosphate buffer) solutions was conducted at a constant pressure of 20 kPa for SG-PES membrane and of 40 kPa for SC cellulose-based membrane (in order to obtain similar initial water flux) for 3 h of filtration. The flux profile over time was monitored online gravimetrically. Thereafter, the solution was removed, and the membrane surface was externally rinsed by two times filling the cell with pure water (25 mL) and shaking it for 30 s.

$$\mathrm{RFR} = \frac{J_0 - J_a}{J_0} \times 100\% \quad (1)$$

Table 1
Observed characteristics of the UF membranes used in this study

Parameter	SG-PES	GR-PES	SC-cellulose-based
Water permeability (L/m^2 h kPa)	0.905 ± 0.106	0.080 ± 0.016	0.468 ± 0.021
Rejection of dextran (T4/T10/T15/T100) (%)	7/78/83/100	20/85/89/100	28/92/96/100
Surface porosity from AFM (%)	13.2 ± 4.4	6.4 ± 4.4	11.0 ± 5.2

2.4. Atomic force microscopy (AFM)

AFM topography images were obtained using a MultiMode AFM with Nanoscope IIIa controller and equipped with a 10 μm scanner from Digital Instruments, Santa Barbara, CA, USA. The tapping mode was applied using an oscillating cantilever with a silicon tip having a radius of <10 nm. Dry membrane samples of about 25 mm^2 area were mounted on a steel disc with double sided sticky tape and subjected to analysis in air under room temperature conditions. The cantilever oscillation was tuned to a frequency between 250 and 325 kHz. For the analysis of morphology, surface porosity and roughness, the AFM image processing program (NanoScope software) was used to zero out waviness of the surface topography. Average roughness (R_a) and root-mean-square roughness (R_{ms}) were obtained at surface areas of 1 μm^2.

2.5. Attenuated total reflection infrared spectroscopy (ATR-IR)

ATR-IR spectroscopy using a Bruker Equinox 55 instrument (Bruker Optics Inc., Billerica, MA, USA) equipped with a liquid nitrogen detector was applied to analyze the surface chemistry of the membrane. A total of 64 scans were performed at a resolution of 4 cm^{-1} using a diamond crystal; the temperature was 21 + 1 °C. A program written for the Opus software from Bruker was used to calculate difference spectra versus the corresponding background spectra.

2.6. Contact angle (CA) and zeta potential (ZP) measurements

CA and ZP experiments were performed for characterization of non-porous PES film. The apparatuses used were the same as in the previous study [1]. CA was measured using sessile drop method, whereas ZP was calculated from data of tangential streaming potential measurements.

2.7. Simultaneous diffusion–adsorption measurements (SDAM)

The SDAM method was used to quantify the amount of solute bound to/in the membrane as well as the effective diffusion coefficient. The diffusion cell consisted of two half-cells, i.e. the upstream cell (high concentration) and the downstream cell (low concentration). Each cell was equipped with a stirring system. The membrane with an effective area of 12.56 cm^2 was placed between the two cells and sealed with O-rings. The upstream and downstream cells were filled at the same time with 120 mL of a solution of either dextran (10 g/L in 0.01 M sodium azide) or myoglobin (400 mg/L, in phosphate buffer pH 7) and 120 mL of either 0.01 M sodium azide solution or phosphate buffer (pH 7), respectively. Even though Lebrun and Junter [11] had reported that for diffusion of dextran through porous media, the mass transfer resistances at the liquid–solid interfaces were negligible, the two half-cells were stirred at the same stirring rate in order to minimize the resistance of boundary layers. The diffusion of the solute through the membrane was monitored by measuring their concentrations in both half cells at certain times for up to 4 h. The effective diffusion coefficient was calculated from the initial diffusion rates, and the amount of solute adsorbed on/in the membrane was deduced from the mass balance.

3. Results

3.1. Effect of dextran molar mass on adsorptive fouling and comparison with adsorptive protein fouling

While in the previous work, dextrans with M_w of 4.5, 9 and 16 kg/mol had been used [1], a much larger variation of average dextran molar mass was performed here. As presented in Fig. 1, it was clearly seen that as the molar mass dextran was increased, the RFR would firstly rise up to molar mass of ~70 kg/mol and beyond that value the RFR data decrease again. In addition, the SG-PES membranes showed a smaller flux reduction at low molar masses, but a larger flux reduction at high molar masses when compared to the GR-PES membranes. For comparison, the SG-PES membrane was also exposed to the myoglobin solution, and much higher RFR was observed, i.e. 58% and ~50% for concentrations of 10 and 1 g/L, respectively.

3.2. Visualization of adsorptive dextran fouling by atomic force microscopy

AFM was used to visualize the membrane morphology before and after exposing to the dextran solution. The results are presented in Fig. 2. Images of the native membranes after washing with water and drying at room temperature were used here in order to take into account the effect of wetting the membranes with aqueous solution and subsequent drying prior AFM onto surface morphology (cf. [10] for a discussion why using dry samples). Results in Fig. 2 first suggest that the SG-PES membrane had greater number of pores per surface area than GR-PES membrane. Second, significant changes in surface morphology were observed for both PES membranes, and increases in heterogeneity were much more pronounced for the GR-PES

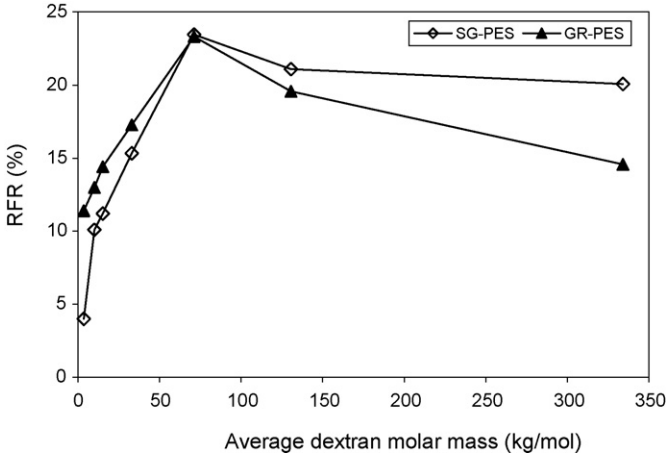

Fig. 1. Effect of dextran molar mass on RFR for PES membranes after static adsorption (solute concentration 10 g/L, time of exposure 3 h).

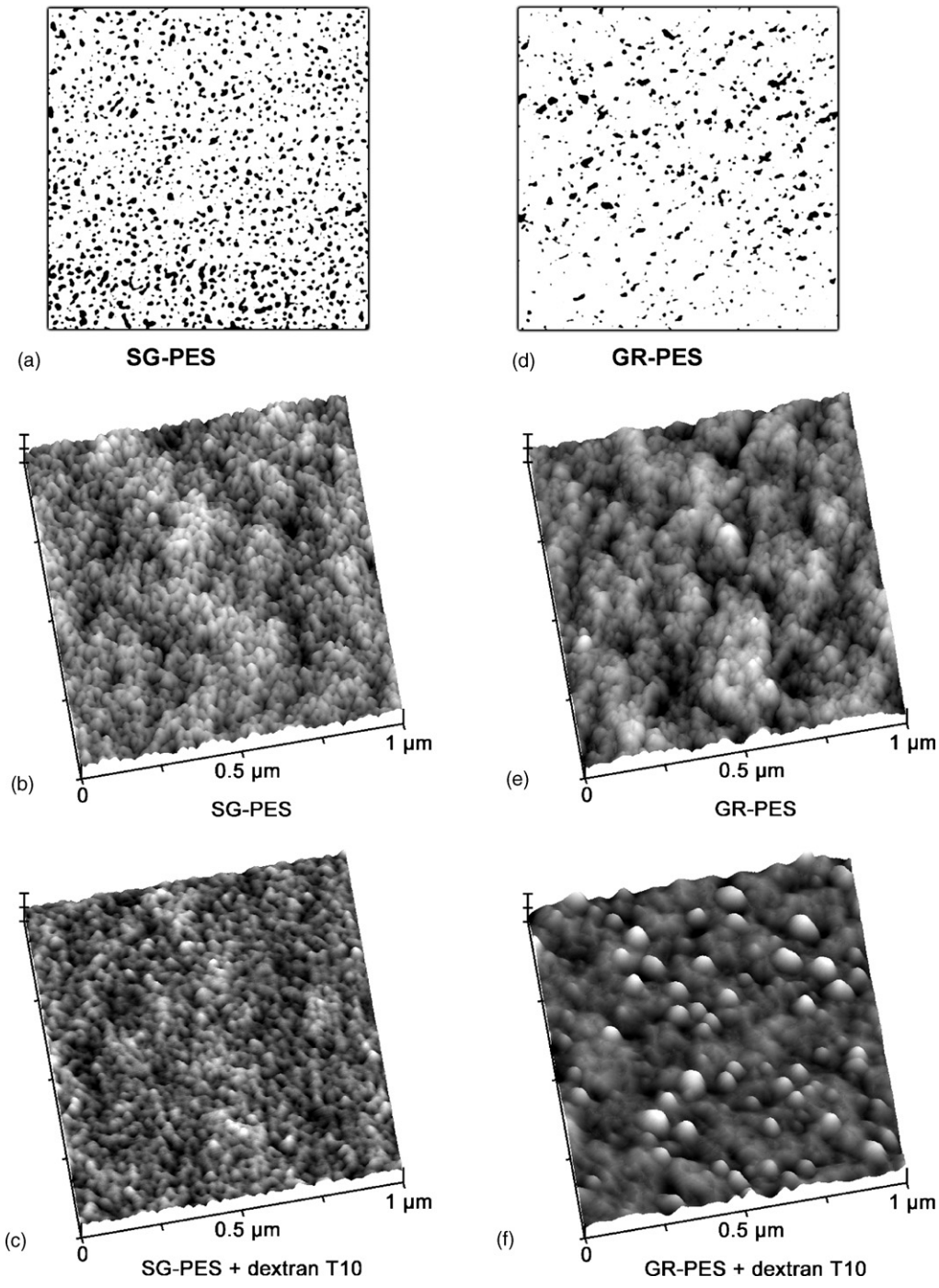

Fig. 2. AFM images of SG-PES and GR-PES membranes and effects of adsorptive fouling on membrane surface morphology. Left: (a) visualization of pores of SG-PES membrane from representative topography images, (b) SG-PES membranes after washing, (c) SG-PES membrane after exposing to dextran T10 solution; right: (d) visualization of pores of GR-PES membrane from representative topography image, (e) GR-PES membrane after washing (f), GR-PES membrane after exposing to dextran T10 solution.

membrane. The average surface roughness (R_a) changed from 0.94–1.12 to 0.64–0.73 nm and from 1.09–1.23 to 1.40–1.51 nm for SG-PES membrane and GR-PES membrane, respectively. The different response with respect to the average surface roughness (decrease for SG-PES and increase for GR-PES) might be due to a difference in structure of adsorbed solute on the membrane surface. These results are qualitatively supported by data of Kweon and Lawler [9]. By using SEM, they observed different surface morphology of fresh and fouled (with dextran) polysulfone UF membranes.

3.3. Characterization of adsorbed dextran using ATR-IR spectroscopy

ATR-IR spectroscopy was used to confirm the dextran fouling on the membrane surface. Both PES membranes showed

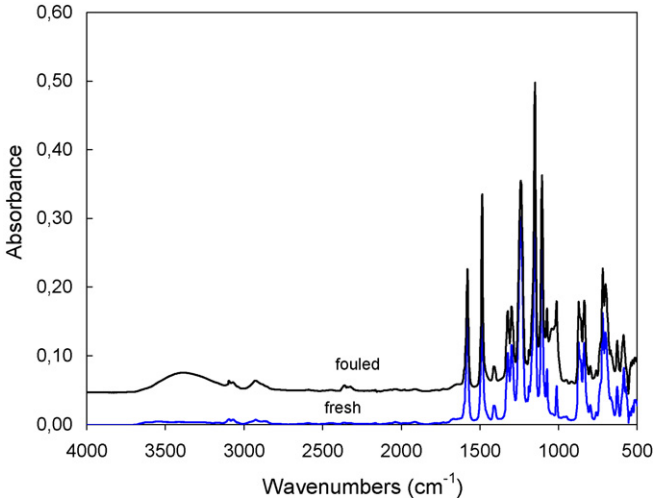

Fig. 3. ATR-IR spectra of fresh and fouled GR-PES membranes (fresh membranes were washed with water, fouled membrane was obtained by exposing to 10 g/L of dextran T10 solution for 3 h).

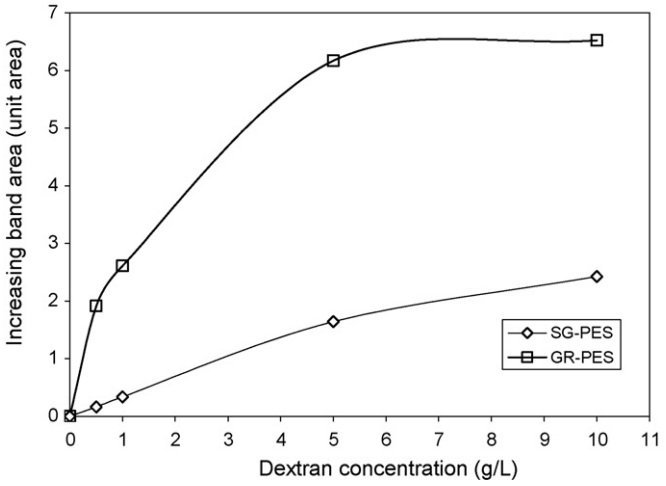

Fig. 4. Increase in ATR-IR band area (in the range 3130–3600 cm^{-1}) for PES membranes after exposing to various concentrations of dextran solution T10 (3 h), relative to ATR-IR spectra for native membranes.

typical aromatic bands at ~1578 and ~1485 cm^{-1} (due to benzene ring C=C bond stretch). Also, the aromatic ether band at around 1240 cm^{-1} was strongly observed. In addition, a significant absorbance band at ~1660 cm^{-1} was found in both PES membranes, and the assignment to a primary amide stretch (CO–NH) was supported by the appearance of another band at ~3360–3340 cm^{-1}. This band was presumably from poly-*N*-vinylpyrrolidone (PVP), which is a well-established additive for the manufacturing of UF membranes from PES. After washing with water, the IR band of this additive was completely absent for the GR-PES membranes but only reduced in intensity for SG-PES membranes (Fig. 3; IR spectra for SG-PES and IR spectra before washing are not shown).

Fig. 3 shows an example of IR spectra of PES membranes before and after dextran adsorption. The observed changes in IR spectra – in the ranges ~3600–3130 cm^{-1} (due to O–H glucosidic groups) and ~3100–2800 cm^{-1} (due to C–H glucosidic groups) – indicate the presence of dextran on the outer membrane surface or in the about 2 μm thick layer sampled by ATR-IR.

Furthermore, a quantitative analysis was done by calculating the absorbance band area (in the range 3600–3130 cm^{-1}) using an integration method and subtracting the respective absorbance band area of the native membrane (after washing with water). As can be seen in Fig. 4, the increase in dextran concentration up to 5 g/L increased the IR band area of the fouled membrane. Beyond that concentration, the increase in band area is slowed down by further increasing the concentration especially for GR-PES membrane. It is also observed that the increase in band area was larger for the GR-PES than for the SG-PES membrane.

3.4. Quantification of adsorbed dextran by simultaneous diffusion–adsorption measurements

SDAM experiments were used to quantify the amount of dextran and myoglobin attached on the membrane as well as their ability to diffuse through the membrane barrier as expressed by the effective diffusion coefficient. In all experiments using dextran T10 and myoglobin, the solute concentration in the high concentration (upstream) half-cell decreased with increasing contact time whereas the solute concentration in the downstream half-cell increased. This indicates that these solutes could penetrate through the pores in the membrane barrier. In contrast, with the dextran T100 no permeation through the membranes could be detected.

The effective diffusion coefficients for various solutes in the two PES membranes are given in Table 2. Dextran diffusion was much faster through the SG-PES membrane when compared to the GR-PES membrane. Diffusion of myoglobin was much slower than diffusion of dextran (measured for the SG-PES membrane). Due to the smaller characteristic pore size of the membranes used for the study, the dextran diffusion coefficients obtained in this study were smaller than those obtained by Lebrun and Junter [11]. The significant difference between the amounts of solute released by the upstream half-cell and received by the downstream half-cell indicates that solute adsorption on or solute binding in the membranes also occurred. The amounts of dextran and myoglobin bound to the membranes as deduced from the mass balance are shown in Fig. 5. After an initial time delay, the bound amount of dextran increased significantly, but beyond a contact time of 3 h the data seemed to approach a plateau value. No significant differences with respect to dextran accumulation on the membrane and effective diffusion coefficient were seen for the same membrane type in inverse orientation. For myoglobin, it was observed that the bound mass increased largely between 0 and 1 h whereas the further increases

Table 2
Effective diffusion coefficients (m^2/s) of dextran and myoglobin through different UF membranes

Membrane	Dextran T10	Dextran T100	Myoglobin
SG-PES	4.8×10^{-12}	No diffusion	9.4×10^{-13}
SG-PES, inverse	5.2×10^{-12}	n.d.	n.d.
GR-PES	2.4×10^{-12}	n.d.	n.d.

n.d.: not done.

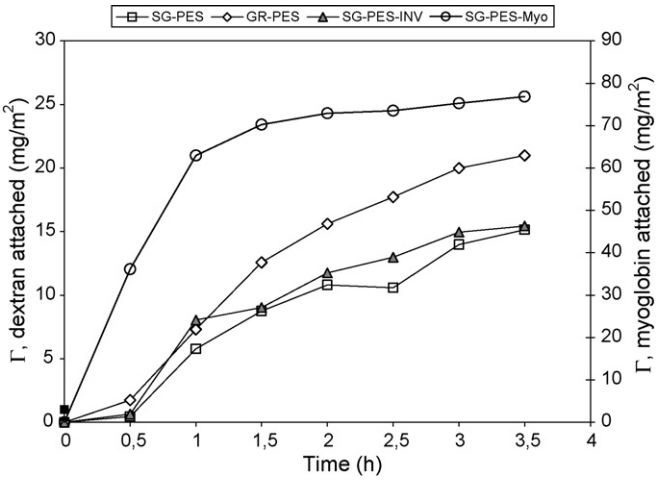

Fig. 5. Amount of dextran and myoglobin bound on/in the PES membranes (dextran T10 concentration 10 g/L, "SG-10-INV" . . . data from diffusion experiment with dextran T10 through membrane in inverted orientation; myoglobin concentration 400 mg/L at pH 7).

between 1 and 2 h were relatively small, and beyond 2 h a plateau condition seemed to be reached (∼75 mg/m^2). Assuming that the available surface area on the membranes is similar for dextran and for myoglobin, the surface coverage by myoglobin is ∼5 times greater than by dextran (calculated from the ratio of bound amounts).

Fig. 6 shows – again for the SG-PES membrane where both time-dependent data were available – that there is a good correlation between the RFR values from pure water flux measurements and the bound dextran amounts obtained from the SDAM experiments.

3.5. Solute adsorption on non-porous PES film surface

In order to eliminate the effect of pore structure on the interaction between solute and membrane surface, additional experiments were done using non-porous PES films. The effects

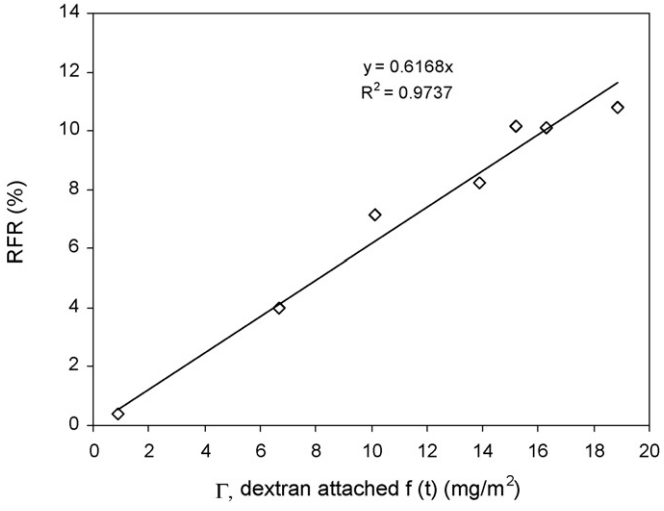

Fig. 6. Correlation between RFR and the amount of dextran attached on membrane as a function of exposure time for SG-PES membranes (dextran T10, 10 g/L).

Table 3
Static contact angles measured by sessile drop method using water of non-porous PES film surface

PES film	After exposing to dextran[a]	After exposing to myoglobin[b]
75.9 ± 2°	71.7 ± 2°	67.0 ± 1.1°

[a] Dextran T10 solution (10 g/L) in water (3 h exposure).
[b] Myoglobin solution (1 g/L) in phosphate buffer pH 7 (3 h exposure).

of adsorption were evaluated by measuring contact angles (Table 3) and zeta potential (Fig. 7).

Overall, exposing the PES film to both dextran and protein solutions reduced the CA and absolute ZP significantly. These CA and ZP reductions for non-porous PES films agree well with results of the previous study using PES UF membranes [1]. The reduction of CA was larger after exposing to the myoglobin than to the dextran. Both biomacromolecules are hydrophilic, and therefore, the apparent hydrophilization of the PES surface strongly indicates solute adsorption. A similar phenomenon, i.e. a decrease in CA after adsorption of a protein (BSA), had also been reported by Swerdya-Krawiec et al. [12]. That the change had been smaller in our study may be related to the smaller and more compact protein. The reduction of negative ZP for pH > 5.8 was larger for myoglobin than for dextran, and for pH < 5.8 the ZP after myoglobin adsorption was even positive. The latter can be explained considering the isoelectric point (IEP) of the myglobin (pH ∼ 7), i.e. an excess of positive surface charge was introduced via the protein.

3.6. Fouling during dead-end stirred ultrafiltration

UF experiments at constant trans-membrane pressure were conducted using both dextran (1 g/L) and myoglobin (0.1 g/L, pH 7) solutions (Fig. 8). It should be noted that the experiments were performed at very low pressure (20 kPa for SG-PES membrane or 40 kPa for SC-membrane) and using 10 times lower solute concentration compared to the conditions used in the

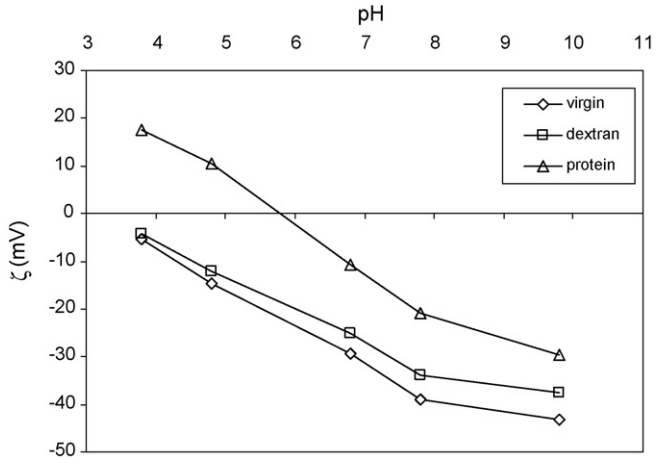

Fig. 7. Zeta potentials (ZP), ζ, calculated from tangential streaming potentials, as a function of pH (using 0.001 mol/L KCl) for non-porous PES film surfaces before and after exposing to the solutions of dextran T10 (10 g/L) and myoglobin (1 g/L) for 3 h.

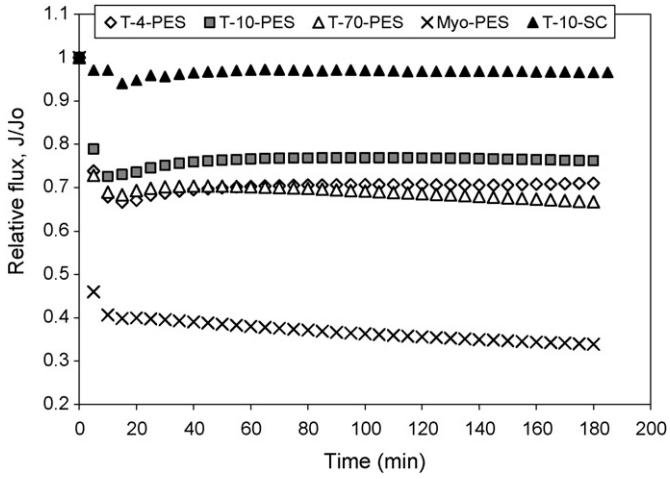

Fig. 8. Flux profile as function of UF time for solution of various dextrans (1 g/L) and myoglobin (0.1 g/L, pH 7) using SG-PES and SC-cellulose-based membranes at a trans-membrane pressure of 20 and 40 kPa, respectively.

Table 4
RFR after ultrafiltration and observed rejection for different solutes with SG-PES and SC-cellulose-based membranes[a]

Solute	SG-PES membrane		SC-cellulose membrane	
	RFR (%)	Rejection (%)	RFR (%)	Rejection (%)
Dextran T4	9.2	35.3	n.d	n.d
Dextran T10	8.2	73.8	~0	82.3
Dextran T70	10.3	99.2	n.d	n.d
Myoglobin	47.0	76.5	n.d	n.d

n.d.: not done.
[a] Some data presented in this table are slightly different from previous results (cf. [1]) due to differences in ultrafiltration conditions.

adsorption/RFR studies. In addition, the solute rejection and the RFR after UF were also measured (Table 4).

The fluxes through the PES UF membrane dropped very rapidly in the beginning of filtration for both dextran and myoglobin solutions. The resulting permeate fluxes were much smaller than the water fluxes. The decreases in fluxes were in the following order: T10 < T4 < T70 ≪ Myo. In contrast, the permeate fluxes for dextran T10 through the cellulose-based membrane were almost identical to the water flux.

The solute rejections during UF were consistent with the differences in (average) solute molar mass (cf. Table 4). The water fluxes through the PES membrane after UF and external rinsing were in all cases significantly smaller than the initial water fluxes, and the RFR for myoglobin was much larger than the respective values for the three dextrans (cf. Table 4). In contrast, for the cellulose-based membrane the original water flux was regained after external rinsing.

4. Discussion

4.1. Membrane–solute and membrane–solute–solute interactions

All data from the different experiments with the PES UF membranes in contact with dextran and protein solutions indicate that there is significant solute binding to the membranes (while dextran binding to the cellulose-based UF membranes appeared to be not significant [1]). Our earlier study also demonstrated significant dextran fouling of PES membranes by filtration experiments (RFR, sieving) and by qualitative changes in surface properties (contact angle and zeta potential) [1]. This study is mainly focused on visualization and quantitative analysis of this dextran fouling in order to identify the mechanism of interaction.

Quantitative data for bound dextran on the PES membranes in contact with a solution (no convective flux through the membrane) were obtained with two different methods. The ATR-IR data showed clearly the influence of dextran concentration, with a plateau beyond 5 g/L (cf. Fig. 4), and this was similar to the concentration dependency of the RFR data (cf. Fig. 2 in [1]). Also, the effects for fouled GR-PES membranes (with T-10 (10 g/L): IR ratio = 6.5, cf. Fig. 4; RFR = 13%, cf. Fig. 1) were larger than for SG-PES membranes (with T-10 (10 g/L): IR ratio = 2, cf. Fig. 4; RFR = 10%, cf. Fig. 1). Hence, the amount of dextran adsorbed on the GR-PES membrane should be higher. Indeed, the bound amounts of dextran T10 obtained from SDAM experiments (after 3.5 h) were larger for GR-PES (21 mg/m^2) than for SG-PES membranes (15 mg/m^2). Again, this result was in line with previous RFR results (cf. Fig. 1 in [1]). It is very important to note that a good correlation was obtained between data for bound dextran and the RFR for the same membranes (cf. Fig. 6).

Further, the bound amount of solute obtained from SDAM was much higher for myoglobin than for dextran (cf. Fig. 5), and this correlated also with a much higher RFR value. These results indicate that myoglobin had a larger affinity than dextran of similar size, that a higher coverage of the accessible membrane surface by the protein (>5 times higher than for dextran) was reached at high solution concentration, and that pore narrowing and blocking were much more severe after protein than after dextran adsorption. A high affinity of protein to PES membranes and large fouling effects had been reported by many other authors (e.g., [13]).

When comparing the correlation of both quantitative methods (SDAM and IR) with RFR data, larger deviations to higher values were observed for the IR method. This could be explained with the surface selectivity of the method (sampling depth into the membrane only about 2 μm); i.e. the accumulation of dextran in the active layer region is selectively detected with this method. In this context, the data for dextran fouling visualization using AFM are very interesting. The changes in surface morphology due to dextran adsorption were significant and much larger for GR-PES than for SG-PES membrane (cf. Fig. 2). The ultimate reason might be the difference in the ability to disperse the dextran on the outer surface during drying (note that drying the membrane with an adsorbed hydrophilic polymer on the surface will also involve dehydration of the hydrophilic polymer and can lead to aggregation). The different behaviour is presumably caused by different surface porosities (cf. Fig. 2(a) and (d)): the lower porosity of the GR-PES membrane leads to a smaller number of larger dextran aggregates (cf. Fig. 2(c) and (f)).

A better correlation of RFR with the SDAM data (cf. Fig. 6) would indicate that solute binding deeper in the selective layer

of the PES UF membrane is also involved in flux reduction. A contribution to the fouling by the penetration of dextran with low molar mass into the pores has already been discussed in our previous study [1]. Because diffusion of the dextran T10 through the membranes was observed and was not influenced by membrane orientation (cf. Table 2), this explanation is reasonable. The complex effects of dextran molar mass on RFR by adsorption to PES membranes (cf. Fig. 1) can then be analyzed based on the relationship of membrane pore size and dextran size. For average molar masses up to 70 kg/mol, bound dextran molecules could either narrow or (completely) block the membrane pores. With increasing ratio between dextran size and pore size the probability for pore blocking will increase. It should be noted that the pore blocking will yield a higher contribution to membrane resistance than pore narrowing [14]. Ye et al. [3] found similar results during their study of cross-flow filtration using alginate, i.e. smaller pore diameters gave a higher resistance caused by fouling. However, beyond a molar mass of 70 kg/mol, the dextran could not penetrate into the membrane pores, as confirmed by complete rejection in UF (cf. Table 1) and no diffusion for the dextran T100 (cf. Table 2). Hence, even though dextran is a flexible coil polymer and is able to deform within the membrane pores [15], the PES membrane pores are too small for dextran of this size. As a result, the extent of dextran fouling was reduced with increasing molar mass. Further, the differences in adsorptive fouling (extent and consequence) between the two PES membranes can again be explained with their different surface morphology (cf. Fig. 2): for the SG-PES membrane with larger surface porosity and average pore size, the effects for smaller dextran size were smaller (less effects of adsorption on pore narrowing), but for larger dextran size they were larger (more effective pore blocking) than for the GR-PES membrane.

The much lower UF permeate fluxes as compared to the water fluxed seemed to indicate that the concentration polarization at the membrane surface was significant during UF with the PES membrane (cf. Fig. 8). However, the small flux decline for the SC membrane shows that concentration polarization was in fact quite low for this membrane (note that the UF was performed at low transmembrane pressure and almost identical initial water flux for both membranes). Consequently, the higher flux decline for the SG-PES membrane was largely caused by fouling. This was also supported by the significant water flux reductions after UF and external rinsing for the PES, but not for the cellulose-based membrane (cf. Table 4). Similar to the effects of static adsorption, the accessibility of the pores for dextran of different size seemed to contribute to the fouling effects as well.

4.2. Mechanism of interactions

Based on the results of this and our previous study [1], it is reasonable that the differences in membrane surface coverage caused by different mechanisms of interaction were the reasons for the different fouling behavior of the two different solutes (dextran versus protein) with the two different membranes (PES versus cellulose-based).

The low binding properties of cellulose-based materials are well known (cf., e.g., [16]), and the fouling resistance of the SC membrane is due to the swollen, hydrogel-like morphology of the UF-selective barrier layer. Mechanisms of interactions between the membrane polymer PES and proteins have been discussed in many phenomenological or mechanistic studies (see, for example, [17,18]). The main driving force at a pH around the isoelectric point of the protein is hydrophobic attraction between PES and protein. However, in contrast, an attractive interaction between the relatively hydrophobic PES and the neutral hydrophilic dextran is counter-intuitive.

It should be noted, that also in the adsorption experiments without convective flux through the membrane (cf. Section 2.3), there is a concentration gradient between the bulk solution and the water in the membrane, i.e. “behind” the active layer. Therefore, it could be possible that the dextran accumulation on/in the membrane is caused by diffusion into the membrane and mechanical entrapment in the pore structure. Such a scenario would be more probable for the smaller dextrans which can penetrate the active layer (cf. Figs. 1 and 5). In order to rule out such effects, additional experiments with non-porous PES films were performed (cf. Fig. 7 and Table 3). Both CA and ZP data clearly indicate that the surface of the PES film have been modified by solute adsorption for protein and dextran, and the surface coverage seemed to be larger for the protein than the dextran. The CA and ZP results for dextran with the non-porous PES films agree well with the previous data for porous PES UF membranes [1]. Therefore, the significant changes in PES surface structure upon contact with dextran solution can only be explained by adsorption of the solute to the polymer surface.

Two possible mechanisms are proposed to contribute to these attractive interactions. First, the binding of dextran to PES can be due to hydrogen bonding between free hydroxyl groups in the dextran (as donor) and oxygen atoms projecting from the SO_2 group in PES (as acceptor). Multiple hydrogen bonds can be formed between one dextran molecule and the membrane polymer surface, and this could provide a significant enthalpy contribution to a negative free enthalpy for adsorption. Second, water structure and reactivity at solid surfaces should also be considered. While binding of water to a hydrophilic surface is too strong to be displaced by a solute [19], the binding of water to hydrophobic surfaces is weaker. The adsorption to hydrophobic surfaces is mainly driven by the increase in entropy via replacement of water molecules at the surface by adsorbed solute (“surface dehydration”) [20]. This process would also provide a contribution to a negative free enthalpy for adsorption of a hydrophilic polysaccharide on a hydrophobic polymer surface.

5. Conclusions

A comprehensive membrane characterization and an analysis of the impact of membrane characteristics on polysaccharide and protein fouling in UF have been performed. The membrane–solute interactions were strongly influenced by the membrane characteristics (cellulose-based versus PES, pore structure) and solute properties (polysaccharide versus protein, solute molecular mass, solute concentration). It was clearly

observed that both protein and polysaccharides were bound to the PES membranes and caused significant fouling. The PES membrane surface coverage by protein was much greater than membrane surface coverage by polysaccharides, and as a consequence fouling caused by protein was also more severe. The experiments using nonporous PES films confirmed that dextran adsorbed to the PES surface with a surface coverage that was lower than for myoglobin. The hydrophobic interaction was the main driving force for PES–protein interaction in this study. Two possible mechanisms, i.e. multiple hydrogen bonding and changes in water structure at the membrane polymer surface, were proposed to explain the attractive PES–dextran interaction. Nevertheless, the pore structure of the membrane skin layer in relation to the average size of the dextran also contributed to the extent of pore narrowing or blocking due to adsorptive fouling. Overall, this work provides fundamental information about a previously overlooked or underestimated problem, and it makes a significant contribution to a better understanding of polysaccharide fouling in general.

Acknowledgements

HS would like to thank the DAAD, Germany, for a Ph.D. scholarship. The authors wish to thank Dieter Jacobi for his valuable help with the GPC analyses and Tim Leimer for her contribution to ATR-IR analysis. The authors would also like to thank Alfa-Laval, Nakskov, Denmark, and Sartorius, Göttingen, Germany, for donation of the membranes.

References

[1] H. Susanto, M. Ulbricht, Influence of ultrafiltration membrane characteristics on adsorptive fouling with dextrans, J. Membr. Sci. 266 (2005) 132.
[2] B.P. Frank, G. Belfort, Polysaccharides and sticky membrane surface: critical ionic effect, J. Membr. Sci. 212 (2003) 205.
[3] Y. Ye, P. Le Clech, V. Chen, A.G. Fane, Evolution of fouling during crossflow filtration of model EPS solutions, J. Membr. Sci. 264 (2005) 190.
[4] A. Vernhet, M. Moutounet, Fouling of organic microfiltration membranes by wine constituents: importance, relative impact of wine polysaccharides and polyphenols and incidence of membrane properties, J. Membr. Sci. 201 (2002) 103.
[5] N.K. Saha, M. Balakrishnan, M. Ulbricht, Polymeric membrane fouling in sugarcane juice ultrafiltration: role of juice polysaccharides, Desalination 189 (2006) 59.
[6] P. Mulherkar, R. van Reis, Flex test: a fluorescent dextran test for UF membrane characterization, J. Membr. Sci. 236 (2004) 171.
[7] R. Nobrega, H.D. Balmann, P. Aimar, V. Sanchez, Transfer of dextran through ultrafiltration membranes: a study of rejection data analysed by gel permeation chromatography, J. Membr. Sci. 45 (1989) 17.
[8] V. Gekas, K.M. Persson, M. Wahlgren, B. Sivik, Contact angles of ultrafiltration membranes and their possible correlation to membrane performance, J. Membr. Sci. 72 (1992) 293.
[9] J.H. Kweon, D.F. Lawler, Investigation of membrane fouling in ultrafiltration using model organic compounds, Water Sci. Technol. 51 (2005) 101.
[10] D. Lazos, S. Franzka, M. Ulbricht, Size-selective protein adsorption to polystyrene surfaces by self-assembled grafted poly(ethylene glycols) with varied chain lengths, Langmuir 21 (2005) 8774.
[11] L. Lebrun, G.A. Junter, Diffusion of dextran through microporous membrane filters, J. Membr. Sci. 88 (1994) 253.
[12] B. Swerdya-Krawiec, H. Devaraj, G. Jacob, J.J. Hickman, A new interpretation of serum albumin surface passivation, Langmuir 20 (2004) 2054.
[13] A. Amanda, S.K. Mallapragada, Comparison of protein fouling on heat-treated poly(vinyl alcohol), poly(ether sulfone) and regenerated cellulose membranes using diffuse reflectance infrared Fourier transform spectroscopy, Biotechnol. Prog. 17 (2001) 917.
[14] G. Belfort, R.H. Davis, A.L. Zydney, The behavior of suspensions and macromolecular solutions in crossflow microfiltration, J. Membr. Sci. 96 (1994) 1.
[15] M.P. Bohrer, G.D. Patterson, P.J. Carroll, Hindered diffusion of dextran and ficoll in microporous membranes, Macromolecules 17 (1984) 1173.
[16] M. Cheryan, Ultrafiltration and Microfiltration Handbook, Technomic Publishing Company Inc., Pennsylvania, 1998.
[17] J.A. Koehler, M. Ulbricht, G. Belfort, Intermolecular forces between a protein and a hydrophilic modified polysulfone film with relevance to filtration, Langmuir 16 (2000) 10419.
[18] A.D. Marshall, P.A. Munro, G. Trägårdh, The effect of protein fouling in microfiltration and ultrafiltration on permeate flux, protein retention and selectivity: a literature review, Desalination 91 (1993) 65.
[19] E.A. Vogler, Structure and reactivity of water at biomaterial surfaces, Adv. Colloid Interface Sci. 74 (1998) 69.
[20] E.A. Vogler, Water and the acute biological response to surfaces, J. Biomater. Sci. 10 (1999) 1015.